Indian Journal of Chemistry
Vol. 64, July 2025, pp. 699-709
DOI: 10.56042/ijc.v64i7.15210

In silico design, molecular docking and synthesis of novel [1,1-biphenyl]-4-carbonitril Schiff base derivatives as cholinesterase inhibitors

Basma M Abd Razik[a], Mohammed Oday Ezzat*[b] & Jessica Shlimoon Hanna[c]

[a] Department of Pharmaceutical Chemistry, College of Pharmacy,
Mustansiriyah University, 10001, Baghdad, Iraq

[b] Department of Chemistry, College of Education for Women, University of Anbar, 31001 Anbar, Iraq

[c] National Diabetes Center, Mustansiriyah University, 10001, Baghdad, Iraq

E-mail: edw.mohamed_oday@uoanbar.edu.iq, basma_m.abd_razik@uomustansiriyah.edu.iq, jessicahanna@uomustansiriyah.edu.iq

Received 21 November 2024; accepted (revised) 1 July 2025

Alzheimer's disease (AD) is a neurodegenerative disorder expected to affect over 80 million people by 2040. A decline in acetylcholine (ACh), a key neurotransmitter, is linked to cognitive decline in AD. Acetylcholinesterase (AChE) and butyrylcholinesterase (BChE) enzymes break down ACh, making them targets for AD treatment. This study aimed to synthesize Schiff base derivatives and evaluate their ability to inhibit AChE and BChE. Molecular docking has been used to explore their binding interactions. Three Schiff base derivatives (**N1**-**N3**) have been synthesized by condensing substituted benzaldehydes with 4-(4'-aminophenyl)benzonitrile. Their cholinesterase inhibitory activity has been tested using a modified Ellman's method, and docking studies have been performed using Glide™. The compounds show strong inhibition of both AChE and BChE. **N1** has the strongest AChE inhibition (IC_{50} = 1.09 µg/mL), while **N3** is most effective against BChE (IC_{50} = 12.32 µg/mL). Molecular docking confirms favorable binding through hydrogen bonding and hydrophobic interactions. *In vitro* and docking results show **N1** and **N3** as potent inhibitors of AChE and BChE. Their interactions with key amino acids supports their inhibitory potential. Novel Schiff base derivatives **N1** and **N3** show promising cholinesterase inhibition. Their dual activity against AChE and BChE positions them as potential candidates for AD treatment. Further studies are recommended.

Keywords: Alzheimer's disease, Molecular docking, AChE, BChE, Schiff base derivatives

Alzheimer's disease (AD) is a prevalent neurodegenerative disorder affecting around 2% of the global population, with an estimated 80 million cases by 2040 (Ref. 1). AD is associated with significant behavioral issues, cognitive deficits, and progressive memory loss, with some of the additional symptoms that may be present[2,3]. AD is a multifactorial disease with unknown causes, characterized by abnormal beta-amyloid (Aβ) accumulation, cholinergic neuron death, metal dyshomeostasis, and other complications[4,5]. One of the main causes is a lack of acetylcholine (ACh) and butyrylcholine (BCh), which are broken down by Acetylcholinesterase (AChE) and Butyrylcholinesterase (BChE), respectively[6,7]. ACh breakdown to choline and acetic acid is inhibited by AChE inhibitors, increasing neuronal ACh [8]. ACh is crucial in facilitating the attention, formation of memories, learning processes, and motivation[9]. Meanwhile, inhibiting cholinesterase enzymes (ChEs) is a key approach to boosting brain ACh[10]. Now there are only 4 drugs classified to cholinesterase inhibitors; rivastigmine, donepezil, galantamine and one other N-methyl-D-aspartate (NMDA) receptor antagonist memantine available to management of AD[11]. Rivastigmine is recognized for its ability to inhibit both AChE and BChE, among the three ChE inhibitors[12]. Active site of AChE is a 20 Å deep gorge, and the catalytic triad contains three amino acids: Ser203, Glu334, and His447, which are essential for activity[13]. The initial interaction between ACh and the acetylcholinesterase enzyme takes place at the outer gorge, which is referred to as the peripheral anionic site (PAS)[14]. This site is composed of Trp279, Tyr70, Tyr121, and Phe290 amino acids[15]. Four primary sub-sites are present at the bottom of the gorge: the acyl pocket, where ACh is hydrolyzed; the esteratic site; the anionic sub-site; and the oxyanion hole[16,17]. Furthermore, the main distinction in structure between AChE and BChE is that BChE

lacks the PAS moiety located at the top of the gorge. Therefore, it is evident that an inhibitor of cholinesterase that strongly interacts with the PAS will have a higher level of selectivity for AChE compared to BChE[18]. The AChE active site exhibits a preference for hydrophobic contacts. Consequently, molecules containing an aromatic ring in their structure provide more favorable interactions[19]. The BChE enzyme substitutes the aromatic rings that are present in the gorge of AChE with aliphatic rings, enabling the binding of bulkier substrates[8,20]. Based on extensive research, the most effective treatment approach for AD is the development of AChEIs, which function on two binding sites of the enzyme and restore cholinergic deficiency by simultaneously interacting with the enzyme's catalytic active site and the PAS to reduce the formation and deposition of Aβ[21]. This research focuses on the synthesis of new Schiff bases and investigates their efficacy as anticholinesterase agents (Fig. 1 and Fig. 2). Molecular docking was then utilized to investigate the plausible binding interactions of the compounds.

Experimental Section

Melting points are uncorrected and were measured with Stuart Scientific (SMP1) equipment. TMS was used as the internal standard and DMSO-D6 as the solvent to record the ^{1}H, ^{13}C- NMR spectra using a Bruker (Avance) 500 MHz NMR equipment. The NMR data processing software utilized was Bruker Topspin 3.0. The coupling constants are expressed in Hertz, while the chemical shifts are expressed in parts per million (d-scale). Elemental analysis was done using Perkin Elmer 2400 instrument series II Elemental CHN analyzer while crystalline studies on compound **N3** were done using a Bruker SMART APEX II CCD area detector.

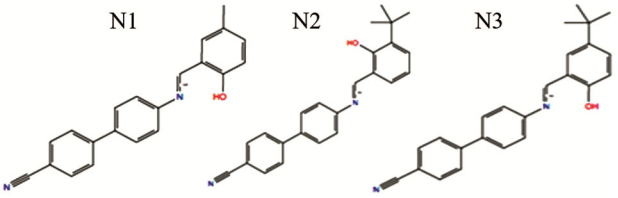

Fig. 1 — structure of newly synthesized compounds

The general synthesis procedure of Schiff bases series N(1-3)

The synthesis of the Schiff bases was carried out by taking equimolar dry mixture of R-substituted benzaldehydes compounds **1-3** and 4-(4'aminophenyl) benzonitrile. 4-Substituted benzaldehydes were obtained by taking 5 mmol of the aldehyde and dissolving in 25 mL of absolute methanol and then slowly adding to equal volume of 4-(4'aminophenyl)benzonitrile dissolved in absolute methanol. The reaction mixture was then heated for 3 h by placing the set up in water bath which acted as a reflux. The reaction mixture was left to react for a certain period of time before the status of the reaction was deemed completion using thin layer chromatography. After that, the solvent was evaporated under the vacuum in order to obtain crude samples of blue and red pigment. The Schiff bases **1-3** were first washed with hexane and then they were recrystallized using toluene resulting in yields in the range 78-89%.

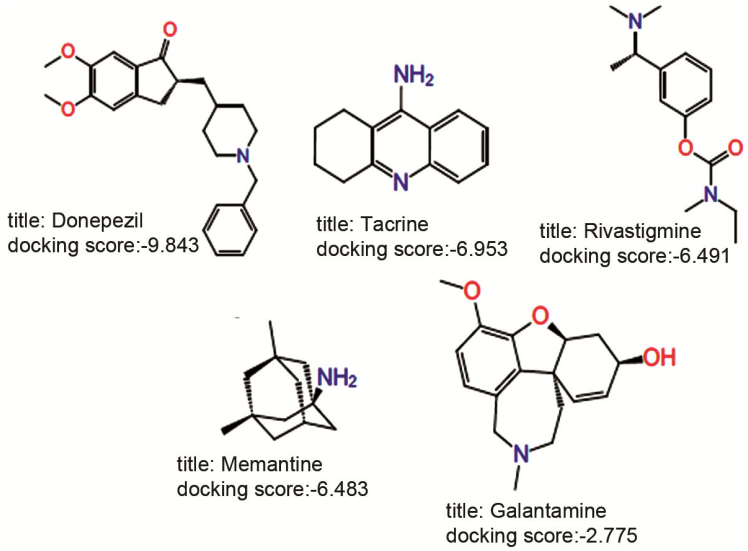

Fig. 2 — A List of docking binding values and chemical structure of acetylcholinesterase inhibitors

Analytical data for (E)-4'-((2-hydroxy-5-methylbenzylidene) amino)-[1,1'-biphenyl]-4-carbonitrile, N1: Yellow solid. Yield 89%. m.p.185-187°C. IR (KBr): 3318, 2232, 1597, 1214 cm^{-1}. Anal. for $C_{21}H_{16}N_2O$; Calcd (found): C: 80.74(80.71), H: 5.17(4.93), N: 8.96(8.94). ^{1}H NMR (500 MHz, DMSO-d_6): δ H 6.89 (1H, d, J = 8.3 Hz, H-3), 7.25 (1H, dd, J = 8.35 Hz, H-4), 7.48 (1H, d, J = 1,8 Hz, H-6). 7.54 (2H, d, J = 8.5 Hz , 3', 5'), 7.87 (2H, d, J = 8.5 Hz, H-2′, H-6′).7.94 (4H, s, H-2″, 3″, 5″, 6″), 8.97 (1H, s, H-7), and 12.69 (1H, s, OH); ^{13}C NMR (125 MHz, DMSO-d_6): δ C 19.90, 109.9, 116.4, 118.8, 119.0, 122.1, 127.3, 127.7, 128.1, 132.2, 132.8, 134.2, 136.4, 143.7, 148.6, 158.1, 163.6.

Analytical data for (E)-4'-((3-(tert-butyl)-2-hydroxybenzylidene) amino)-[1,1'-biphenyl]-4-carbonitrile, N2: Orange solid. Yield 80%. m.p.191-193°C. IR (KBr): 3318, 2229, 1590, 1213 cm^{-1}. Anal. for $C_{24}H_{22}N_2O$; Calcd (found): C: 81.27(81.31), H: 5.93(6.24), N: 7.92(7.92). ^{1}H NMR (500 MHz, DMSO-d_6): δ H 1.42(9H,s,CH_3), 6.94. (1H, d, J = 8.3 Hz, H-5), 7.41 (1H, dd, J = 8.32 dd, Hz, H-4), 7.51 (1H, d, J = 1,7 Hz, H-6,), 7.89. (2H, d, J = 8.6 Hz , 3', 5'), 7.89 (2H, d, J = 8.5 Hz, H-2′, H-6′),7.94 (4H, s, H-2″, 3″, 5″, 6″), 9.05. (1H, s, H-7), 14.11 (1H, s, OH); ^{13}C NMR (125 MHz, DMSO-d_6): δ C 29.61, 109.9, 118.5, 122.2 127.3, 128.1, 130.4, 131.5, 132.8, 136.51, 136.59, 143.7, 147.8, 159.1, 165.1.

Analytical data for (E)-4'-((5-(tert-butyl)-2-hydroxybenzylidene) amino)-[1,1'-biphenyl]-4-carbonitrile, N3: Orange solid. Yield 78%. m.p.192-194°C. IR (KBr): 3312, 2226, 1593, 1213 cm^{-1}. Anal. for $C_{24}H_{22}N_2O$; Calcd (found): C: 81.27 (81.34), H: 6.03(6.29), N: 7.94 (7.95); ^{1}H NMR (500 MHz, DMSO-d_6): δ H 1.33 (9H,s,$(CH_3)_3$), 6.82 (1H, d, J = 8.3 Hz, H-3), 7.23 (1H, dd, J = 8.32 dd, Hz, H-4), 7.71. (1H, d, J = 1,7 Hz, H-6), 7.88 (2H, d, J = 8.6 Hz, 3', 5'), 7.89 (2H, d, J = 8.5 Hz, H-2′, H-6′),7.92. (4H, s, H-2″, 3″, 5″, 6″), 8.95 (1H, s, H-7), 12.11. (1H, s, OH); ^{13}C NMR (125 MHz, DMSO-d_6): δ C 30.61, 34.21, 111.3, 118.4, 122.6, 127.7, 128.4, 132.3, 134.5, 134.8, 136.53, 137.59, 142.70, 148.70, 159.20, 165.10.

In vitro cholinesterase enzymes inhibitory assay

Using an altered version of Ellman's technique, the inhibitory activity of cholinesterase enzymes was assessed, as reported by Ahmed and Gilani. To use as positive control compound, galantamine was employed. Test sample and galantamine solutions were prepared in DMSO at an initial concentration of 1 mg/mL (equivalent to 1000 ppm). The final reaction mixture contained 1% of DMSO. DMSO does not inhibit the AChE and BChE enzymes at this dosage. In the acetylcholinesterase (AChE) inhibitory experiment, a 96-well microplate was first filled with 140 µL of *p*H 8 0.1 M sodium phosphate buffer, then 20 µL of test samples compounds and 20 µL of 0.09 units/mL acetylcholinesterase enzyme. Following a 15-minute incubation time period at 25 °C, 10 µL of 10 mM 5,50-dithiobis-2-nitrobenzoic acid (DTNB) and 10 µL of 14 mM acetylthiocholine iodide were added to each well. Using a BioTek instrument PowerWave X 340 Microplate Spectrophotometer, the absorbance of the colored end product was measured 30 minutes after the enzymatic process started at 412 nm. The same protocol as previously described was employed for the butyrylcholinesterase (BChE) inhibitory assay; however, butyrylcholine esterase samples from horse serum and S-butyrylthiocholine chloride samples were used in place of the enzyme and substrate. Every test was run three times. The test samples' absorbance was adjusted by deducting the absorbance of the corresponding blank. To compute percentage inhibition, the following formula was used:

$$\text{Percentage of inhibition} = \frac{\text{Absorbance of control - Absorbance of Sample}}{\text{Absorbance of Control}} \times 100$$

Molecular docking studies

The docking study has been performed in this work using Glide™ from the Schrödinger suite (Schrödinger, LLC, New York, NY, 359, 2011) in its version 5. The most active synthesized compounds were positioned at the active site pocket of *Torpedo californica* acetylcholinesterase (TcAChE) which was obtained from the crystal structure of the enzyme when bound to donepezil the anti-Alzheimer compound. Amongst these were the most active synthesized compounds which was predicted to bind onto the active site of TcAChE based on the crystal structures of the enzyme bound to the Alzheimer's anti-drug donepezil. All the interactions were predicted at the molecular interface between the complexes 1EVE and 4EY7, as well as at the active site pocket of human butyrylcholinesterase (hBChE), where the structure was solved in complex with the substrate BCh from the Protein Data Bank entries 1P0P and 6EQP). In addition to excluding waters and

hetero groups outside the 5 Å sphere of the reference ligand compound (donepezil or BCh) around the enzyme, additional cleaning steps were performed. Structure was subsequently relaxed, and it was further reduced by applying Protein Preparation Wizard TM on the basis of the OPLS-2005 force field. Both TcAChE and hBChE grids were compiled from the Receptor Grid Generation programmer. All the ligand files available in the study were prepared using LigPrepTM which involved the conformational generation of each ligand followed by its minimization using the OPLS-2005 optimization force field. In order to simplify the graphic representation of the results, the bioactive compounds were subjected to docking stimulations so as to generate five poses for each ligand; the single best poses with the best score have been represented for each compound.

Results and Discussion

Chemistry

Based on the previous work[21] three new Schiff base derivatives N(1-3) was synthesized *via* condensation of substituted benzaldehyde with 4-(4'-aminophenyl) benzonitrile. Schiff bases N (1-3) formulated from the condensation reaction of equimolar ratio of substituted benzaldehydes with primary amine (4-(4'-aminophenyl) benzonitrile) were heated in the presence of organic solvent absolute methanol, as demonstrated in Fig. 1. Characterization of Schiff bases N (1-3) was done by IR, ^{1}H and ^{13}C NMR spectroscopy and technical elemental analysis CHN. The analysis of ^{1}H NMR spectra for compound **N1** displayed peak for H-3 appear at 6.89 ppm as doublet. The proton of H-4 showed at 7.25 ppm as a doublet of doublets, while the H-6 appear at 7.48 ppm as doublet. The second compound **N2** showed the sharp singlet at 1.42 ppm of $(-CH_3)_3$ group, the doublet of H-5at 6.94 ppm, at 7.41ppm appear the doublet of doublets of H-4, the doublet of H-6 at 7.51 ppm. This signal is typical of three equivalent methyl groups connected to a quaternary carbon and the fact that it is a singlet multiplicity proves that there are no adjacent protons to couple with. Also the signal assigned to the aromatic proton H-3 of the substituted salicylaldehyde ring, which is *ortho* to the hydroxyl group and *meta* to the azomethine functionality. The final compound **N3** the characteristic feature was the appearance of sharp singlet at 1.42 ppm of $(-CH_3)_3$ group, the doublet of H-5 at 6.94ppm. The doublet of doublets of H-4 at 7.41ppm, and the doublet at 7.51 ppm of H-6. X-ray crystallographic diagram for compound **N3** is shown in Fig. 3 and Fig. 4. The structures of new compounds are shown in Fig. 1.

Cholinesterase inhibitory activity

The cholinesterase inhibitory activity of all newly developed compounds was assessed against the enzymes butyrylcholinesterase (BChE) and acetylcholinesterase (AChE). The cholinesterase inhibitory activities of synthesized compounds **N1-N3** were determined against the tested enzymes used in the present at a concentration recorded at 10 µg/mL. Subsequently, IC_{50} values of each series of compounds were calculated referring to the screening outcomes. The results of the acetycholinesterase inhibitory activities **N1**:1.09 µg/mL, **N2**: 2.02 µg/mL and **N3**: 2.30 while Galanthamine: 2.09. The results for butyrylcholinesterase (BChE) includes **N1**: 13.39 µg/mL, **N2**: 1534 µg/mL and **N3**: 12.32 while Galanthamine :19.43.

Molecular docking

The synthesized compounds in this study were successfully docked into the active sites of AChE and BChE enzyme, which was based on the crystalline form of *Torpedo californica* AChE and human BChE, respectively. Fig. 1 and Fig. 2 listed the standard drugs used in this study as a positive control for comparison. Molecular docking calculations were also carried to assess the binding modes of the synthesized Schiff base derivatives (**N1-N3**) in the active sites of acetylcholinesterase (AChE) and butyrylcholinesterase (BChE). Glide 100 –6.7 against crystal structures of AChE (PDB IDs: 1EVE and

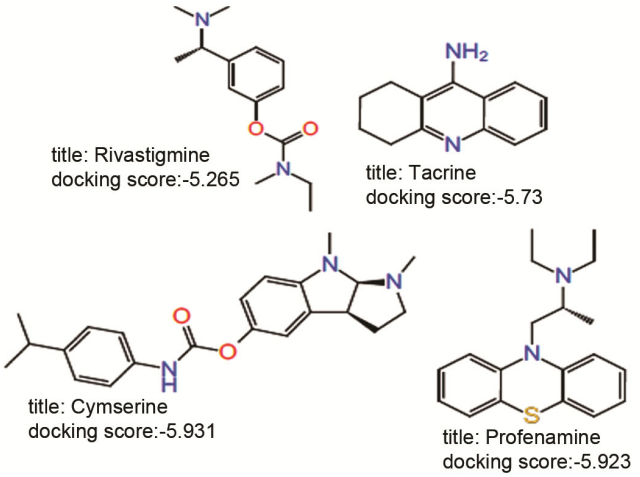

Fig. 3 — A list of docking binding values and chemical structure of butyrylcholinesterase inhibitors

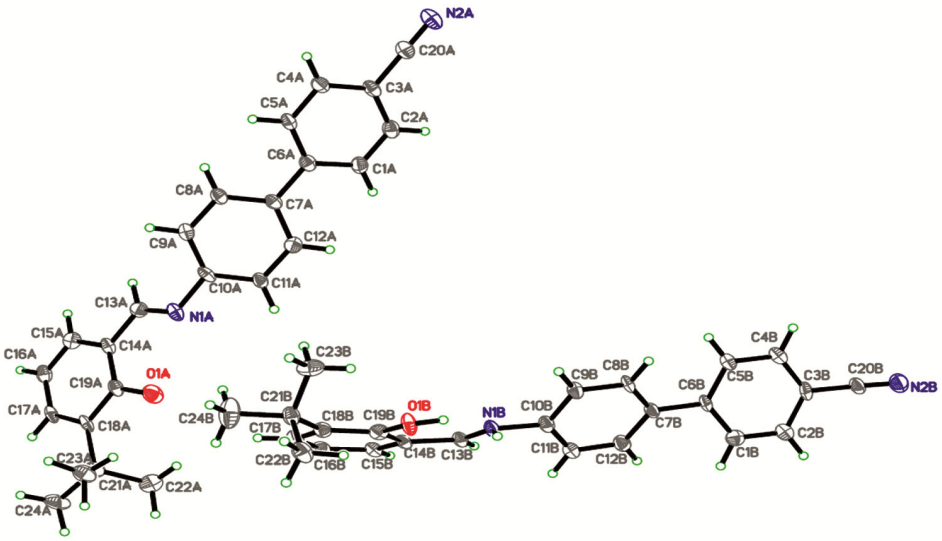

Fig. 4 — The X-ray crystallographic diagram as single view of compound **N3**

4EY7) and BChE (PDB IDs: 1P0P and 6EQP) was used to perform the docking. Docking of the compounds was done using their geometry-optimized structures, and the preparation of receptor grids excluded the water molecules and heteroatoms more than 5 A radius around the reference ligand. The aim of the docking studies was the correlation of the *in vitro* activity as cholinesterase inhibitor with the molecular interactions at the molecular level within the active gorge of these enzymes.

Multiple hydrogen bond interactions along with hydrophobic contacts have occurred between amino acids and chemicals in the active site, resulting in increased favorability of binding. The essential interactions within the active site of AChE with the binding of compound **N1** involve a hydrogen bond between the OH group of the ligand and the amino acid Tyr337. Additionally, pi-pi interactions are formed with the aromatic rings of Tyr341 and Trp86. Furthermore, there are hydrophobic interactions with several amino acids, including Phe295, Val294, Arg296, Phe297, Trp86, Ser203, Glu202, Gly120, Gly121, Gly122, Tyr124, Tyr337, Phe338, Tyr341, and Trp286. In contrast, compound **N2** achieved the highest docking score, with a binding energy of -9.637 kcal/mol, but its interaction profile differs.

Compound **N2** forms pi-pi interactions with Tyr334, Phe330, and Phe331, and also forms hydrogen bonds with two water molecules within the active site. The interactions between the synthesized compound **N1** and the amino acids in AChE differ from those of the reference drug **N2**. Compound **N1** primarily forms hydrogen bonds with Tyr337 and pi-pi interactions with Tyr341 and Trp86, while compound **N2** engages with different amino acids (Tyr334, Phe330, and Phe331) *via* pi-pi interactions and forms additional hydrogen bonds with water molecules. This difference in binding profiles reflects the unique interaction mechanisms of each compound with the active site of AChE.While the hydrophobic interactions were with amino acids Glh199, Ser81, Gln74, Asp72, Tyr70, Gly335, Tyr334, Phe330, Phe331, and Tyr442.

Compound **N3** established a pi-pi contact with Tyr337. Hydrophobic interactions were observed involving the amino acids Gly335, Tyr334, Phe331, Phe330, His440, Asp72, Tyr70, and Ile275. Compound **N1** interacts with the active site of AChE through a hydrogen bond between the OH group and Tyr334.The pi-pi interaction with tyr341 and trp86. Hydrophobic interactions were Phe297, Arg296, Phe295, Trp286, Tyr341, Phe338, Tyr337, Tyr124, Gly122, Gly121, Gly120, Ser203, Glu202, and Trp86. Compound **N2** binds by two pi-pi interactions with phe338, and tyr337. The hydrophobic interactions were phe295, arg296, phe297, phe338, and Tyr337, His447, and Trp86. Whereas, compound **N3** formed hydrophobic interactions with Gly122, Gly121, Gly120, Ser125, Trp86, Tyr337, Phe338, Tyr341, Phe297, Arg296; Phe295, Val294, and Ser293, as long as the highest docking score was –6.341 kcal/mol. with this type of protein. Meanwhile, for BChE (PDB ID: 6EQP), the OH group of compound **N1** binds by H-bond with the amino acid Ala328.

The other hydrophobic interaction was done with the amino acids Gly439, His438, Met437, Ala328,

Phe329, Trp430, Tyr332 and Ser287. However, compound **N2** hydrophobic interaction includes binding with Val280, Ala277, Asn289, and Ser287. The aromatic ring of compound **N3** forms a pi-pi interaction with Trp82. The hydrophobic interaction formed with the amino acids Tyr440, Gly439, His438, Met437, Met434, Gly78, Ser79, Trp82, Ala277, Glu276, Asn289, Ser287, Thr120, and Glu119. Compound **N3** gives the highest binding score (6.341 kcal/mol) with BChE.

In the case of BChE (PDB: 6EQP), the best docking score was observed with compound **N3** (–6.341 kcal/mol) which made 2 3-D interactions, 2 Pi-pi with Trp82, a residue equivalent to Trp86 in AChE, and hydrophobic interactions with Tyr440, Met437, and Gly439. The hydrogen bond between **N1** and Ala328 and favorable hydrophobic contacts explained the binding of **N1**, whereas **N2** showed the least binding (–4.054 kcal / mol), with only partial 6 - interactions and an inadequate fit in the larger gorge of BChE. The observed IC_{50} values agree well with the docking scores: **N3** was the most effective BChE inhibitor and **N1** the most effective AChE inhibitor. such results indicate that dual activity may be justified by positive interactions at both PAS and CAS sites. In general, docking study supports the SAR trends *in vitro* and adds weight to the importance of hydroxyl and aromatic groups in promoting cholinesterase selectivity inhibition.

The **N (1-3)** compounds located inside the active site of the human notum hydrolase active site (PDB ID: 7BDD) exhibit hydrophobic interactions with the amino acids Gly127, Trp128, Tyr129, Ser232, Thr236, and Phe319, Phe320, and Ile291.The compound **N2** exhibited a pi-pi interaction with the amino acid residues Tyr129 and Trp128. Finally, molecule **N3** forms a hydrogen connection with the amino acid Thr236 by binding to the OH group. In addition to the pi-pi interaction involving Trp128. Furthermore, the molecule achieved a docking score of –8.081 kcal/mol, which is the highest value obtained with this active site as displayed in Table 1.

Table 1, Table 2, Table 3 and Table 4 listed the docking results and binding energies of the synthesized Schiff base derivatives **N1-N3** in relation to typical AChE (*e.g.*, donepezil, galantamine) and BChE inhibitors. Direct comparison indicates that compound **N1** displays a docking score of –9.09 kcal/mol with AChE (PDB ID: 4EY7), which is similar or slightly more than the docking score of galantamine (about –8.0 to –8.5 kcal/mol in the literature reports). It indicates that **N1** binds with high affinity especially at the peripheral anionic site (PAS) and catalytic anionic site (CAS) and the important residues involved are Trp86, Tyr337 and Tyr341 which are also usually implicated in the binding of donepezil and galantamine.

In the case of BChE, **N3** docked with a score of –6.341 kcal/mol which is also comparable to that of standard inhibitors such as rivastigmine or galantamine which usually dock with scores ranging between –5.5 to –6.5 kcal/mol. **N3** makes important 3- pi-pi stacking interactions with Trp82 and hydrophobic interactions with residues like Tyr440, Met437 and Gly439, mimicking those made by galantamine. This interaction profile confirms the observed *in vitro* IC_{50} of 12.32μg/mL of **N3** compared to the galantamine IC_{50} of 19.43 μg/mL in similar assay conditions indicating stronger BChE inhibition.

The Schiff bases, especially **N1** and **N3**, utilize both the binding affinity and interaction profiles that are comparable or better than those of standard cholinesterase inhibitors overall. The favorable hydrophobic and -interactions and hydrogen bonding with phenolic -OH and imine functionalities are likely to increase their performance. These data qualify the prospect of Schiff base scaffolds as dual-binding site cholinesterase inhibitors and offer a structural explanation of their biological activity.

Compound **N3** was further analyzed by single-crystal X-ray diffraction (SC-XRD) to give conclusive structural validation to the results and aid the structure activity relationship (SAR) results (Fig. 4 and Fig. 5). Although spectral methods like NMR and IR can provide considerable data on functional groups and connectivity, SC-XRD is the only method that provides a direct way to visualize the molecular geometry, intramolecular interactions and the spatial distribution of substituents. Compound **N3** was the most active against butyrylcholinesterase (BChE) inhibition (IC_{50} = 12.32 mg/mL) among the synthesized Schiff bases and showed the best docking score with BChE (–6.341 kcal/mol), which is likely to be an optimal conformation to interact with biology. Thus, it was important to clarify its native 3D structure to comprehend the conformational preferences that could contribute to binding affinity in enzyme active site. Besides, the presence of stiff aromatic architectures and functional groups with hydrogen bonding abilities justified accurate

Table 1 — 2D and 3D docking results of Schiff base compounds **N1**–**N3** inside the AChE active site (PDB ID: 1EVE)

Compd	3D view of compounds inside active site	2D view of compounds inside active site	Docking Score in kcal/mol	RMSD
N1	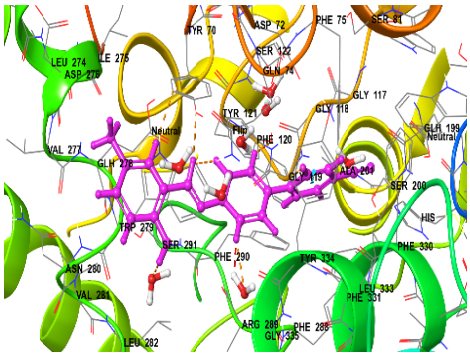	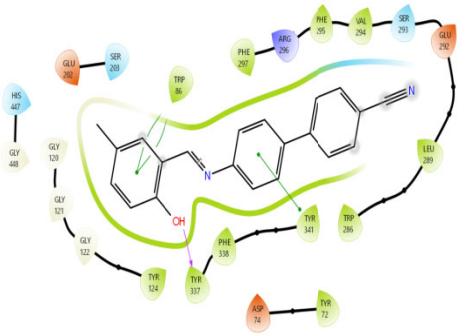	–8.719	94.565
N2	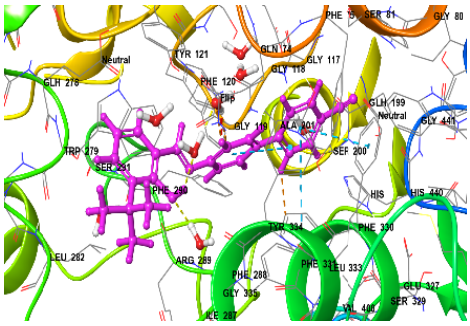	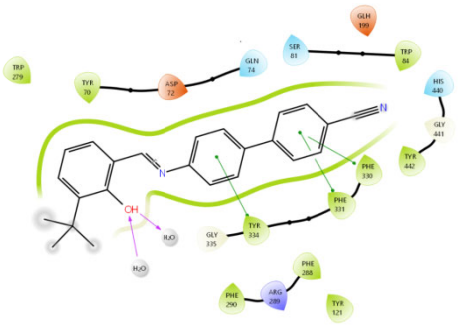	–9.637	96.207
N3	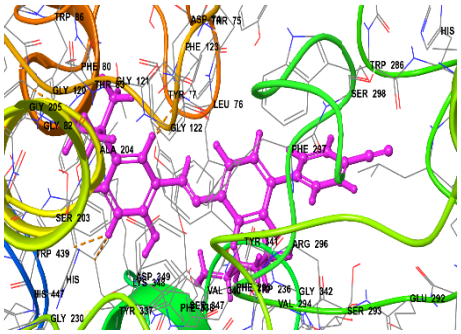	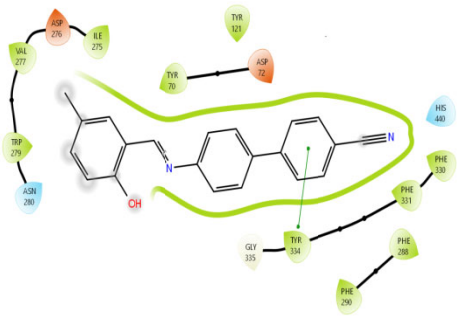	–8.302	96.008

Table 2 — 2D and 3D docking results of Schiff base compounds **N1**–**N3** inside the AChE active site (PDB ID: 1EVE)

Compd	3D view of compounds inside active site	2D view of compounds inside active site	Docking Score in kcal/mol	RMSD
N1	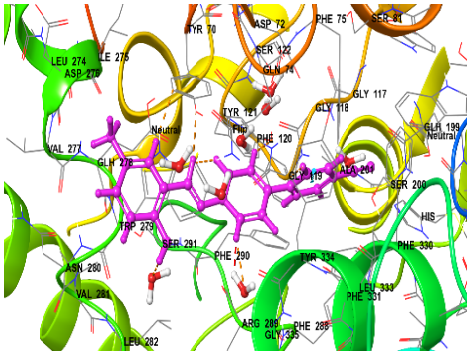	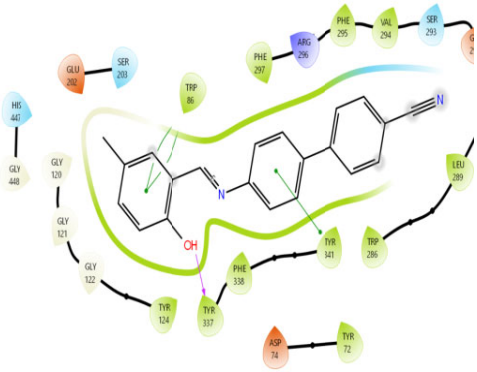	–8.719	94.565

(*Contd*.)

Table 2 — 2D and 3D docking results of Schiff base compounds **N1**–**N3** inside the AChE active site (PDB ID: 1EVE) (*Contd*.)

Compd	3D view of compounds inside active site	2D view of compounds inside active site	Docking Score in kcal/mol	RMSD
N2	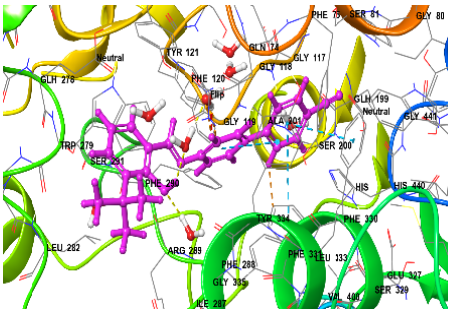	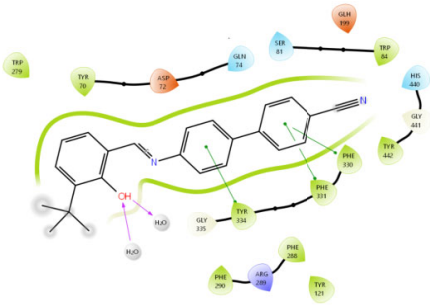	–9.637	96.207
N3	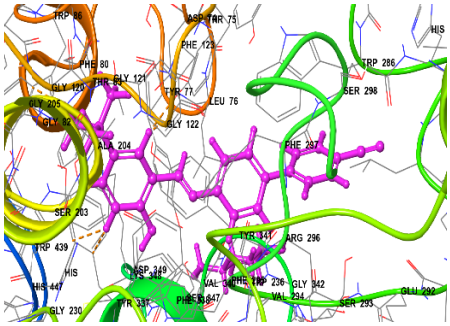	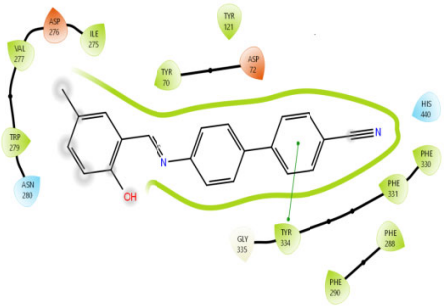	–8.302	96.008

Table 3 — 2D and 3D docking results of Schiff base compounds **N1**–**N3** inside the butyrylcholinesterase (BChE) active site (PDB ID: 6EQP)

Compd	3D view of compounds inside active site	2D view of compounds inside active site	Docking Score in kcal/mol	RMSD
N1	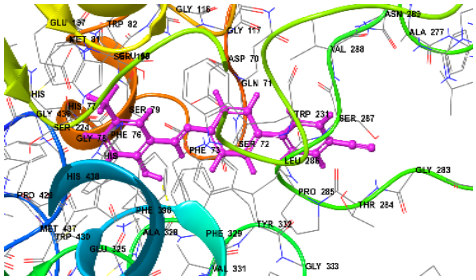	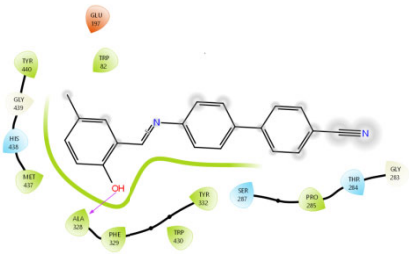	–5.593	66.741
N2	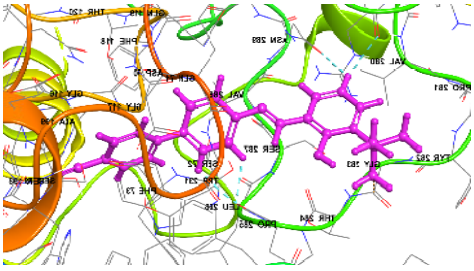	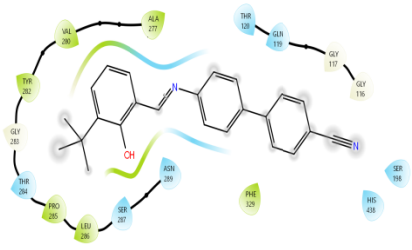	–4.054	64.649
N3	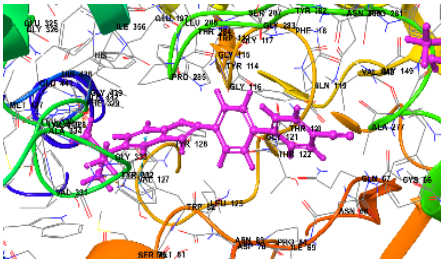	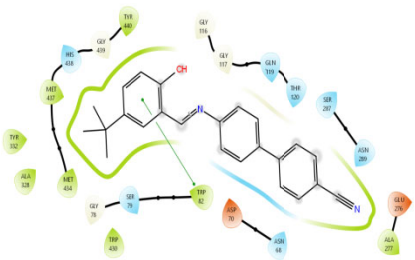	–6.341	63.476

Table 4 — 2D and 3D docking results of Schiff base compounds **N1**–**N3** inside the Notum fragment active site (PDB ID: 7BDD)

Compd	3D view of compounds inside active site	2D view of compounds inside active site	Docking Score in kcal/mol	RMSD
N1	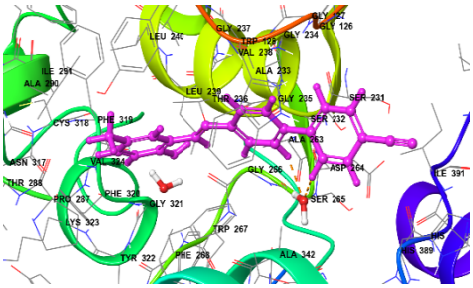	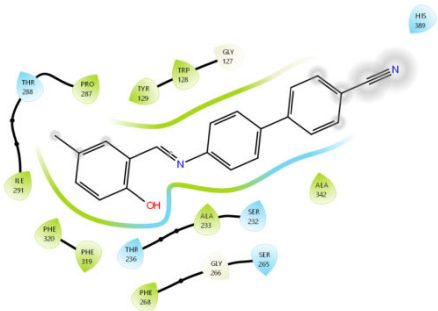	–7.297	13.811
N2	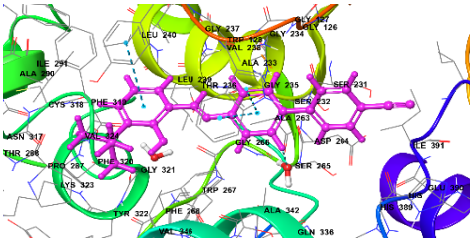	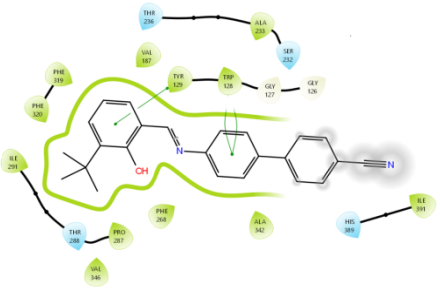	–7.598	14.160
N3	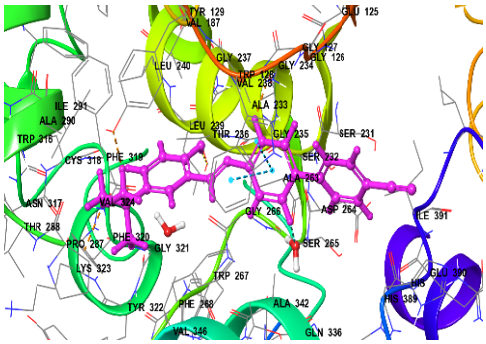	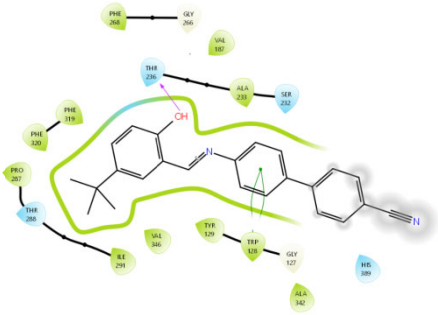	–8.081	14.630

geometric information to support suggested binding positions gained in molecular docking studies. Another effect of the crystal structure is future computational work, such as molecular dynamics and QSAR modeling which will be eased by the availability of high-resolution atomic coordinates. Accordingly, communication of the crystallographic investigation of **N3** is an essential move in linking experimental bioactivity with structural determinants in addition to directing the rational advancement of subsequent generations of cholinesterase inhibitors.

Fig. 4 and Fig. 5 show compound **N3**: its structure and conformation in the solid state were unambiguously confirmed by the single-crystal X-ray diffraction (SC-XRD) analysis. The crystal was solved in monoclinic system with sharp geometry and thermal parameters which supported the molecular formula $C_{24}H_{22}N_2O$ which was supported by

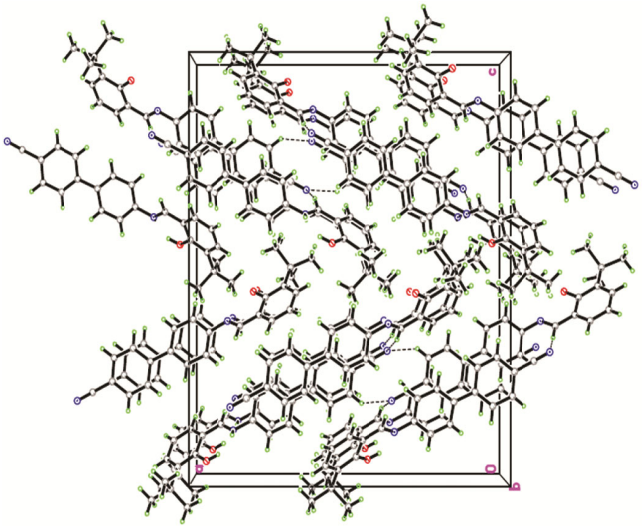

Fig. 5 — The X-ray crystallographic diagram packed view of compound **N3**

elemental analysis. The formation of the Schiff base was evident by the imine (-CH=N-) linkage which was observed with a bond length of about 1.28-1.30 Å. The crystal structure also revealed planar orientation of azomethine and the nearby aromatic rings that allow pi-conjugation, which agrees well with the deshielded singlet at δ 8.95 ppm in the ^{1}H NMR spectrum attributed to the imine proton (H-7).

Notably the phenolic -OH group was observed to be involved in intramolecular hydrogen bonding with the nitrogen of the imine group to give a six-membered pseudo-ring (S(6) motif), which stabilizes the conformation of the molecule. This is captured in the down field chemical shift of OH signal in the ^{1}H NMR spectrum (δ 12.11 ppm), which implies a strong hydrogen bonding. Steric hindrance and crystal pack ing forces result in small angle deviations between the torsion angles about the central bi phenyl system, but overall conjugation is retained.

The tert-butyl group at the 5-position of the salicylidene ring takes up the anticipated staggered confirmation and adds steric bulk and lipophilicity to the molecule. This substituent is also a sharp singlet at δ 8 1.33 ppm in the NMR spectrum and it integrates to 9H, as expected of its chemically identical methyl groups. Moreover bond lengths and angles in the crystal structure are well matched with those anticipated in the optimized geometry utilized in the molecular docking experiments further substantiating the credibility of the computational models. It may be concluded that the crystal structure of **N3** not only validates the successful synthesis and structure of the Schiff base, but also gives important information on the intramolecular interactions, conformation, and geometry which are pertinent to observed biological activity and docking behavior of this compound.

As described in the results, the synthesized compounds were docked into the active sites of acetylcholinesterase (AChE) and butyryl–cholinesterase (BChE), and molecular docking confirmed favorable binding interactions, particularly for compounds **N1** and **N3**. These compounds showed strong *in vitro* inhibition of both AChE and BChE, with **N1** having the strongest AChE inhibition (IC_{50} = 1.09 µg/mL) and **N3** being most effective against BChE (IC_{50} = 12.32 µg/mL). Additionally, docking studies demonstrated key interactions such as hydrogen bonding and hydrophobic contacts within the enzyme active sites. While both methods—docking and *in vitro* testing—identified **N1** and **N3** as the most promising inhibitors, the study did not conduct a detailed comparison or statistical analysis between the docking scores and the IC_{50} values. Future research should aim to correlate these *in silico* and *in vitro* results to establish a clearer relationship and to validate the predictive accuracy of the molecular docking approach in identifying potential drug candidates.

Conclusion

In the present work, three new Schiff base derivatives (**N1**-**N3**) were effectively prepared through condensation reaction of substituted salicylaldehydes with 4-(4-aminophenyl)benzonitrile. Elemental analysis, FT-IR, and ^{1}H/ ^{13}C NMR spectroscopy proved the chemical structures of these compounds. Particularly, compound **N3** crystal structure was elucidated by single-crystal X-ray diffraction, which directly revealed its molecular geometry, intramolecular hydrogen bonding, and planarity, which are aspects that can be easily related to its experimentally observed biological activity.

In vitro inhibitory activity against acetylcholinesterase (AChE) and butyrylcholinesterase (BChE) as major therapeutic targets in Alzheimer's disease was tested with all synthesized compounds. Compound **N1** was the most potent AChE inhibitor (IC_{50} = 1.09 g/mL) compared to the standard drug galantamine. Conversely, Compound **N3** displayed the most potent inhibition of BChE (IC_{50} = 12.32 µg/mL) indicating that it may be a dual-target inhibitor. Molecular docking studies substantiated these results and indicated high binding affinity energies and crucial interactions, including π - stacking and hydrogen bonding with critical active site residues, especially in the PAS and CAS of the cholinesterase enzymes.

A combination of crystallographic information, spectral studies, and docking modeling studies has presented a solid structure–activity relationship (SAR) explanation to the inhibitory action of these Schiff bases. The simultaneous inhibition of two enzymes by the compounds **N1** and **N3** observed indicated that these could be lead scaffolds in the design of multitarget-directed ligands (MTDLs) in the treatment of Alzheimer. Next efforts should be directed towards *in vivo* pharmacology, blood-brain barrier permeability and structural optimization to further

enhance potency, selectivity and pharmacokinetic parameters.

Supplementary Information

Supplementary information is available in the website http://nopr.niscpr.res.in/handle/123456789/58776.

References

1 Hasan A H, Abdulrahman F A, Obaidullah A J, Alotaibi H F, Alanazi M M & Noamaan M A, Murugesan S, Amran S I, Bhat A R & Jamalis J, *Pharmaceuticals*, 16 (2023) 971.

2 Simunkova M, Alwasel S H, Alhazza I M, Jomova K, Kollar V, Rusko M & Valko M, *Arch Toxic*, 93 (2019) 2491.

3 Avram S, Udrea A M, Nuta D C, Limban C, Balea A C, Caproiu M T, Dumitrascu F, Buiu C & Bordei A T, *Molecules*, 26 (2021) 4160.

4 Gutti G, Kakarla R, Kumar D, Beohar M, Ganeshpurkar A, Kumar A, Krishnamurthy S & Singh S K, *Eur J Med Chem*, 182 (2019) 111613.

5 Makhaeva G F, Kovaleva N V, Rudakova E V, Boltneva N P, Grishchenko M V, Lushchekina S V, Astakhova T Y, Timokhina E N, Serkov I V, Proshin A N, Soldatova Y V, Poletaeva D A, Faingold I I, Mumyatova V A, Terentiev A A, Radchenko E V, Palyulin V A, Bachurin S O & Richardson R J, *Int J Molecular Sciences*, 24 (2024) 321.

6 Kausar N, Murtaza S, Arshad M N, Munir R, Saleem R S Z, Rafique H & Tawab Abdul, *J Mol Struc*, 1244 (2021) 130983.

7 Ghafary S, Ghobadian R, Mahdavi M, Nadri H, Moradi A & Akbarzadeh T, Najafi Z, Sharifzadeh M, Edraki N, Moghadam F H & Amini M, *DARU J Pharm Sci*, 28 (2020) 463.

8 Nicolet Y, Lockridge O, Masson P, Fontecilla-Camps J C & Nachon F, *J Bio Chem*, 278 (2003) 41141.

9 Kısa D, Korkmaz N, Taslimi P, Tuzun B, Tekin Ş, Karadag A & Sen F, *Bioorg Chem*, 101 (2020) 104066.

10 Şahin, Ö, Ü Özmen Özdemir, N Seferoğlu, Ş Adem, and Z Seferoğlu, *J Biomol Struc Dyn*, 40 (2022) 4460.

11 Zanon V S, Lima J A, Cuya T, Lima F R S, Fonseca A C C D, Gomez J G, Ribeiro R R, Franca T C C & Vargas M D, *J Inorg Biochem*, 191 (2019) 183.

12 Makhaeva G F, Boltneva N P, Lushchekina S V, Rudakova E V, Serebryakova O G, Kulikova L N, Beloglazkin A A, Borisov R S & Richardson R J, *Bioorg Med Chem*, 26 (2018) 4716.

13 Silva C H T P D, Campo V L, Carvalho I & Taft C A, *J Mol Graph Model*, 25 (2006) 169.

14 Dvir H, Silman I, Harel M, Rosenberry T L & Sussman J L, *Chem-Bio Interact*, 187 (2010) 10.

15 Kryger G, Silman I & Sussman J L, *Structure*, 7 (1999) 297.

16 Peitzika S C & Pontiki E, *Molecules*, 28 (2023).

17 Driant T, Nachon F, Ollivier C, Renard P Y & Derat E, *Chem Bio Chem*, 18 (2017) 666.

18 Larik, FA, MS Shah, A Saeed, HS Shah, PA Channar, M Bolte & Iqbal J, *Int J Bio Macromol*, 116 (2018) 144.

19 Sussman J L, Harel M & Silman I, *Chem-Bio Interact*, 87 (1993) 187.

20 Basiri A, Razik B M A, Ezzat M O, Kia Y, Kumar R S, Almansour A I, Arumugam N & Murugaiyah V, *Bioorg Chem*, 75 (2017) 210.

21 Amin K M, Rahman D E A, Allam H A & El-Zoheiry H H, *Bioorg Chem*, 110 (2021) 104792.